

NUMERICAL SIMULATION OF REINFORCED CONCRETE DETERIORATION

E. J. Hansen and V. E. Saouma
Dept. of Civil, Environmental & Architectural Engineering,
University of Colorado, Boulder, CO 80309-0428, USA

Abstract

Within the context of a numerical study of concrete bridge deck deterioration, simulation of chloride diffusion, steel corrosion, and concrete cracking are investigated. Chloride diffusion and reinforcing steel corrosion are shown to be easily modeled through the diffusion model generally available in most commercial finite element codes, whereas cracking is handled by a special nonlinear fracture mechanics program.

Keywords: Concrete Deterioration; Steel Corrosion; Concrete Fracture; Chloride Diffusion; Finite Elements.

1 Introduction

The deterioration of highway bridges in general, and deck deterioration in particular are well documented, Jones (1995), Weyers et al. (1994). Since deck deterioration manifests itself primarily through cracking and spalling as a result of chloride induced rebar corrosion and expansion, the authors have undertaken a comprehensive investigation of this problem through numerical simulation.

The numerical simulation of bridge deck deterioration due to

chloride-induced rebar corrosion is broken down into three steps.

1. Diffusion of chlorides into the concrete, which breaks down the environment in the concrete and allows corrosion to begin.
2. Electrochemical corrosion of rebar, when an electric circuit is created and corrosion product formed.
3. Fracture of the concrete due to the pressure caused by the corrosion product.

This process is graphically shown in Fig. 1.

The first phase of the numerical simulation consists of a transient finite element analysis of the diffusion of chloride through the concrete. The result of this first phase is the determination of chloride concentration at the rebar as a function of time. This, in turn, will be used to determine the location and initial potentials of anodes and cathodes on the rebar.

The second phase consists of a finite element analysis of the electrochemical corrosion process. Starting with the anodic and cathodic potentials determined from the conditions present at the end of phase one, the finite element analysis is performed to determine the potential field at all other points and its gradient, which is current density. The current density is related to the corrosion rate, which is the amount of rust produced around the rebar over time.

The third phase consists of a stress analysis of the concrete to determine the location and propagation of cracks caused by the rebar corrosion, which manifests itself as a volume increase around the rebar. The boundary conditions for the stress analysis are provided by the results of phase two, with the volume expansion acting as the natural boundary conditions. The results of phase three are the location and size of corrosion-induced cracks over time.

2 Chloride diffusion analysis

Mangat et al. (1992) states that chloride diffusion directly affects concrete deterioration and the onset of steel corrosion by breaking down the passivity of the reinforcing steel and acting as a catalyst in the corrosion reaction itself. The chloride concentration at which steel passivity is broken is called the critical chloride concentration.

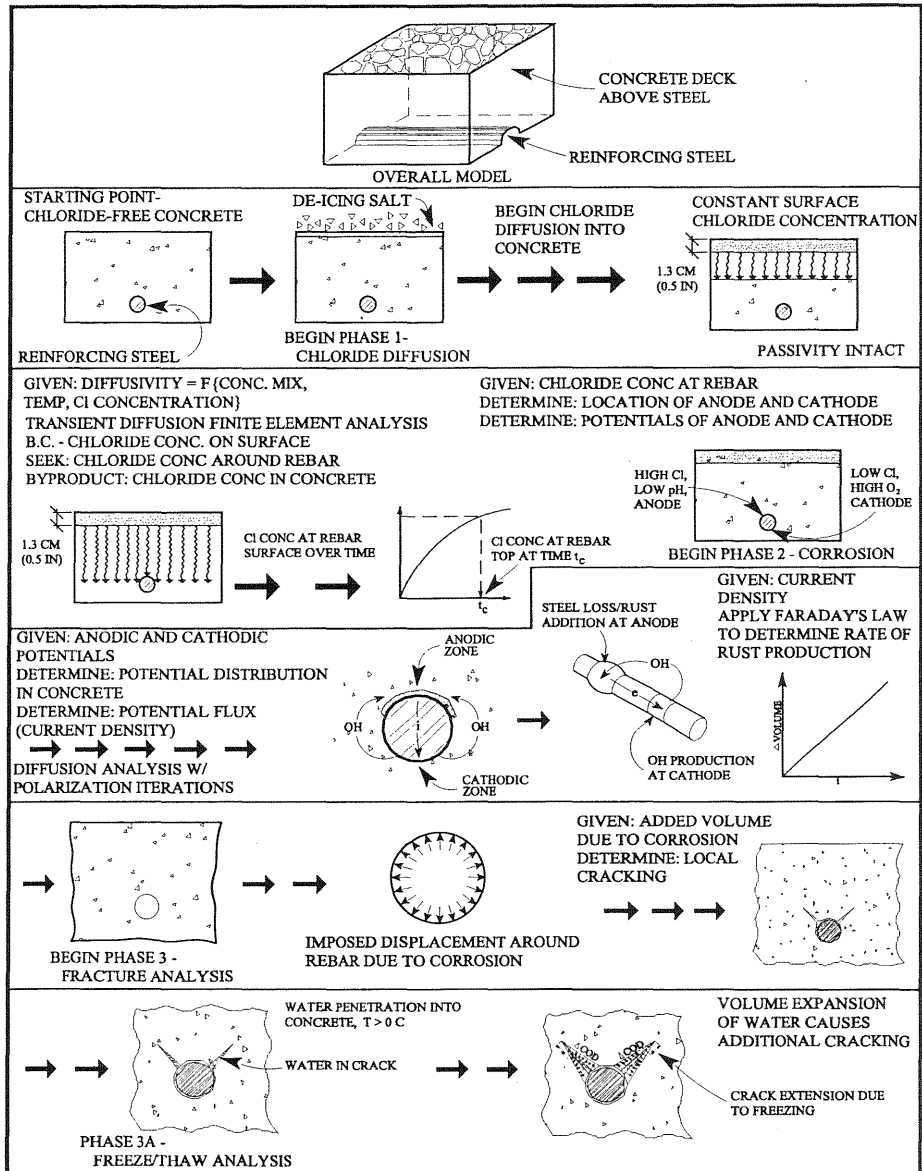


Figure 1: Outline of the Bridge Deck Deterioration Model

The goal of the chloride diffusion analyses is to determine the time to reach this critical concentration of chloride ions at the rebar.

The mass diffusion capabilities of the commercial finite element code ABAQUS (1995) are used here to complete the chloride dif-

fusion analyses. ABAQUS applies a modified version of Fick's law so that diffusion analyses can include the effects of temperature on mass diffusion. In all analyses, a constant chloride concentration was applied to a horizontal plane approximately 1.3 cm below the concrete surface, following the conclusion by Weyers et al. (1994) that chloride concentration in bridge decks is relatively stable at this depth. The analyses were run incrementally in order to determine the chloride concentrations in the deck at different times.

Initial ABAQUS results with simply a constant diffusivity coefficient were found to match those of the closed-form analytical solution of Weyers et al. (1994). The analyses were then improved with the addition of a time decay function by Mangat et al. (1994) to decrease the diffusivity with time. These results agreed with those of the closed-form solution developed by Mangat et al.. Further analyses then departed from closed-form solutions with the addition of temperature effects, which can be included by modifying the concrete diffusivity, D , according to Arrhenius' law, Tang et al. (1994). These temperature-dependent diffusion analyses were preceded by thermal analyses to determine the temperature throughout the deck. The thermal analyses included the effects of air temperature, solar radiation, and surface irradiation. The final analyses performed involved both the time decay function and the temperature effects to obtain a diffusion analysis dependent upon both time and temperature.

The results of these finite element analyses showed that indeed the chloride concentration in a bridge deck can be determined over time. These analyses can include the effects of time and temperature on the concrete diffusivity. Most importantly, the results show that these analyses can determine the time to reach the critical chloride concentration at the rebar.

3 Electrochemical corrosion simulation

Once the critical chloride concentration is reached at the rebar, the passivity of the rebar is broken and active corrosion begins. The parts of the rebar which are depassivated become anodic, while the rest of the rebar becomes cathodic. Corrosion in a closed system

is characterized by the Laplace equation, $\nabla^2\Phi = 0$, where Φ is the potential. Since corrosion is simply an exchange of ions between anodes and cathodes, it can be modeled using the mass diffusion capabilities of ABAQUS. Polarization at the steel/concrete interface requires an iterative approach to the solution.

It was assumed that the top of the rebar acted as the anode while the rest of the rebar was cathodic. This was assumed because the top of the rebar will be the first to experience a high chloride concentration and thus lose its passivity, becoming anodic. Initial potentials were then placed at the anodic and cathodic nodes in the FE mesh. The diffusion analysis was then performed to determine the potential distribution and the fluxes in the mesh. Current density, i , is determined by the equation $i = k\nabla\Phi$, where k is the conductivity of the electrolyte that the current is moving through. Since the current density is simply the gradient of the potential, current density is equal to the flux in a mass diffusion analysis.

Polarization at the steel/concrete interface is characterized by the equation $\phi = E_{oc} + R_p i$, where ϕ is the new potential after polarization, E_{oc} is the open-circuit potential, and R_p is the polarization resistance. The anodic and cathodic potentials are then updated using this relation, and a new diffusion analysis performed. This iterative procedure of determining the potential distribution and current density and then updating the anodic and cathodic potentials according to the polarization relation is continued until the anodic and cathodic current densities converge to constant solutions. Since rust forms around the anodic areas of a rebar, the anodic current density is a measure of the corrosion rate.

Once the corrosion rate is determined, the rate of rust production around the rebar can be determined using Faraday's law, $r = ia/nF$, where r is the corrosion rate (rust thickness per unit time), i is the current density, a is the atomic weight, n is the number of equivalents exchanged, and F is Faraday's constant. Thus the result of the corrosion simulation is the corrosion rate in rust thickness per unit time.

4 Concrete fracture analysis

As rust is produced, it gradually builds pressure around the reinforcing steel because rust occupies more volume than steel. This buildup of pressure will eventually crack the concrete around the steel, and the crack or cracks will propagate with further increased pressure. If the cracks propagate to the surface, the concrete will begin breaking off, or spalling. Mechanical loads, hydrostatic pressure, and freeze/thaw can contribute to the cracking and spalling. As shown in Fig. 4, cracking in bridge decks may be in the vertical,

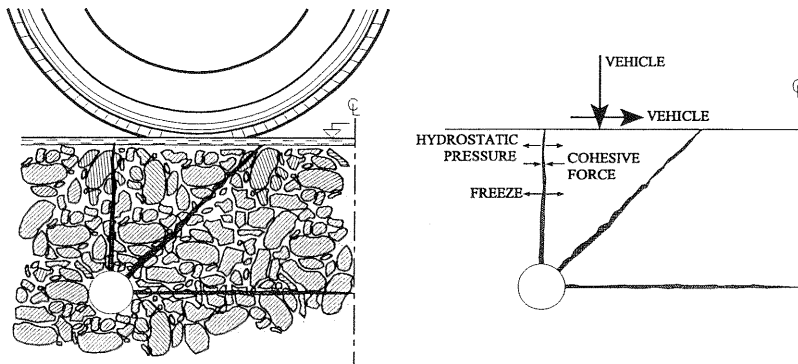


Figure 2: Different loads for bridge deck fracture

horizontal, or diagonal directions.

Bazant (1979) concluded that there are two types of failures in bridge decks: spalling and delamination. Spalling is a result of diagonal cracks reaching the concrete surface, and delamination is a result of horizontal cracks bridging between adjacent rebars. Bazant determined that these two failure modes are a function of the rebar spacing. In particular, he gave two equations:

$$s > 6D \quad \text{Inclined cracking occurs} \quad (1)$$

$$L > (s - D)/2 \quad \text{Horizontal cracking occurs} \quad (2)$$

where s is the rebar spacing, D is the rebar diameter, and L is the depth of concrete cover.

The fracture of concrete can be characterized using the principles of non-linear fracture mechanics (NLFM). MERLIN (1994), a finite

element analysis program with NLFM capabilities, has been developed at the University of Colorado at Boulder by Reich, Červenka, and Saouma. Using MERLIN, the size and location of cracks in bridge decks due to reinforcing steel corrosion can be determined.

4.1 MERLIN concrete fracture analysis

MERLIN adopts the discrete crack approach based on Hillerborg's fictitious crack model (FCM) Hillerborg et al. (1976). Cracking begins when the maximum principal stresses exceed the tensile strength of the concrete, f'_t . A bilinear softening model is adopted to model the concrete stiffness at stresses above f'_t . The area in which this bilinear softening occurs is called the fracture process zone (FPZ). Stresses are transferred across the crack in this zone. The FPZ ends at a point when the crack opening displacement (COD) exceeds a set limit. Above this limit, stresses are no longer transferred across the crack, and a true crack is formed.

While cracks in concrete initiate as pure mode I (tensile), or crack opening, they can propagate as mode II cracks (shear), or crack sliding. However, Hillerborg's FCM only deals with mode I cracks. To account for both tensile and shear cracking, MERLIN uses the interface crack model (ICM) developed by Červenka (1994). The basis for the ICM are interface crack elements. Crack opening and sliding may occur between the two sides of the interface elements.

The fracture analysis proceeds in an incremental manner by first inserting a short path of interface elements in the direction of the maximum principal stress at a node. An analysis is then run to determine if indeed a crack will propagate along the interface. If it is determined that the crack propagates, more interface elements are inserted in the direction of the crack, and the process is repeated. In this incremental way changes in the crack direction can be followed.

4.2 Bridge deck fracture analyses - trial 1

The first set of fracture analyses assumes five crack paths: two horizontal, two diagonal (45°), and one vertical crack extending from the rebar. While vertical cracks extending downward from the rebar may exist, it is assumed that these cracks will not affect the spall

or delamination of the concrete deck. Rebars are assumed to be spaced at 203.2 mm (8 in) centers. The rebar itself is modeled as a void in the FE mesh, and displacements are applied at each node in a direction normal to the void. The applied displacements are equal to the corrosion rate, in thickness per time, determined in the corrosion analyses. The rest of the boundary conditions are roller supports at the bottom and sides, and a free condition at the top of the mesh. The complete mesh, with interface elements, is shown in Fig. 3. The applied radial displacement in the rebar void is equal

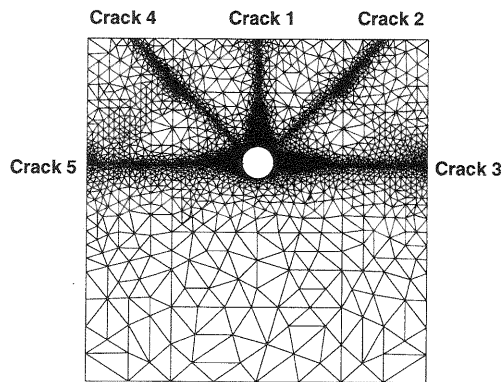


Figure 3: FE mesh for trial 1 – 4631 nodes

to 0.00136 mm per increment, which, at a corrosion rate of 0.012 mm/yr, gives a time of 41.6 days per increment. Due to the large computation time required for this analysis, 30 increments are used, which equals a total time of about 3.4 years.

The results show that the two diagonal and horizontal crack paths propagate symmetrically, as expected. While the analysis does not run long enough for true cracks to form, the crack paths do open up enough to form FPZ's. The FPZ's of the horizontal crack paths reach the edge of the FE mesh after 2.0 years, while the FPZ's of the diagonal and vertical crack paths do not reach the edge. The two diagonal crack FPZ's stop propagating after 1.5 years, while the vertical crack FPZ stops when the horizontal FPZ's reach the edge of the mesh. The normal stress at the tip of the vertical FPZ is positive until the horizontal FPZ's reach the FE mesh edge. At

this point the stress becomes negative, stopping any further vertical propagation. It seems that a stress redistribution takes place as the horizontal FPZ's near the edge of the FE mesh, and this redistribution first halts the diagonal FPZ propagation and then halts the vertical propagation.

4.3 Bridge deck fracture analyses - trial 2

While the results of the previous analysis seem acceptable, the lingering question is whether the assumed crack paths are correct or if the cracks move at different angles. To answer this question, a new set of analyses was performed. These analyses assume no crack paths. Instead, the analysis is run incrementally, adding new interface elements where and when needed. The analysis begins with a "clean" mesh (no interface elements) with the same roller B.C. as the trial 1 analysis and with applied displacements equal to 0.000272 mm per increment, giving an increment time of 8.3 days each at 0.012 mm/yr. The maximum principal stresses at the nodes around the rebar void are then examined. If the maximum principal stress exceeds f'_t , interface elements are inserted in the direction of the maximum principal stress to a length of 10 mm.

After about 21 days of displacement at 0.000272 mm/day, the maximum principal stress at the top of the rebar exceeds f'_t . Interface elements are inserted in the vertical direction since that is the direction of the maximum principal stress. A second analysis is begun with the vertical crack, and after 36 days the diagonal cracks at the upper half of the rebar appear. However, unlike the previous analysis, the diagonal cracks are at 36° . More interface elements are inserted, and a new analysis begun. This iterative procedure of adding cracks continues, and finally at 56 days the horizontal cracks appear. Also, two diagonal cracks appear at the lower half of the rebar, pointed in a direction 18° below horizontal. The FE mesh now has seven crack paths, all 20 mm long.

With seven crack paths identified, the analysis now continues with applied displacements of 0.00272 mm, giving an increment size of 83 days. Each time the maximum principal stress at each crack tip exceeds f'_t , additional interface elements are inserted at lengths of

10 mm each. This gives good control over the direction of the cracks, since every 10 mm the crack path can change direction. The upper diagonal cracks follow angles of $33 - 38^\circ$ while the lower diagonal cracks follow angles of $18 - 23^\circ$. The vertical crack remains vertical, and the horizontal cracks remain roughly horizontal.

At time $t=1160$ days, all the crack FPZ's reach the edge of the concrete surface. The FE mesh at this stage is shown in Fig. 4.

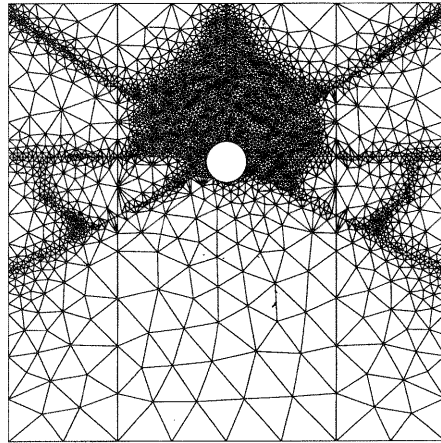


Figure 4: FE mesh for trial 2 - 5008 nodes

A total analysis time of 34 years is now considered to determine when the COD's open enough to form true cracks. The results after 34 years show that only the horizontal cracks form true cracks over their entire length. The vertical crack ligament only has a true crack for the first 30 mm from the rebar. The two upper diagonal crack COD's are only large enough for true cracks over the first 10 mm of their ligaments. The two lower diagonal cracks only have true cracks for the first 40 mm of their ligaments. Since only the horizontal cracks open true cracks over their entire length, it can be concluded that these cracks dominate the deck fracture, forming a plane of delamination between rebars.

4.4 Bridge deck fracture analyses - trial 3

The analyses of trials 1 and 2 consider a 203.2 mm rebar spacing. Trial 3 considers a rebar spacing of 101.6 mm (4 in) to determine

how the rebar spacing affects crack opening. Trial 3 uses the same crack pattern as trial 2, except that the lower diagonal cracks are removed. The FE mesh is shown in Fig. 5.

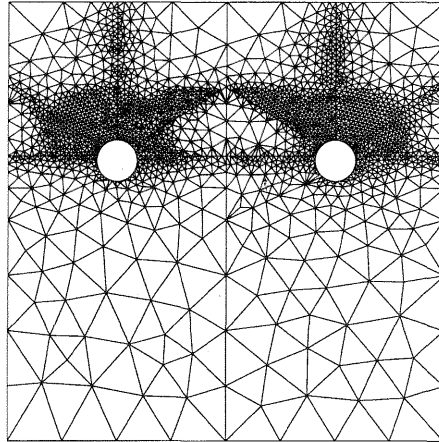


Figure 5: FE mesh for trial 3 – 3068 nodes

The total analysis time is again 34 years. The results show that both the diagonal cracks and the horizontal cracks have true cracks over their entire lengths. The crack tip stresses for these cracks indicate further crack opening past this 34 year analysis. This is a distinct change from the results of trial 2, in which the diagonal cracks do not form true cracks over their entire lengths.

Since the diagonal cracks are full true cracks, it can be concluded that diagonal cracks dominate the deck fracture for this geometry. While both the horizontal and diagonal cracks are true cracks, the diagonals meet above the horizontals and form diagonal spall planes. The diagonal spall planes lead to more concrete damage than the horizontal delamination planes, and thus the diagonal cracks are the dominating cracks for this geometry.

4.5 Results comparison for trials 2 and 3

Since analyses 2 and 3 resulted with true crack patterns, their results can be compared to Bažant's dominant crack pattern assumptions given by Eqs. 1 and 2.

Trial 2 has a rebar spacing $s = 203.2$ mm (8 in), bar diameter $D = 18.75$ mm (0.738 in), and concrete cover $L = 63.65$ mm (2.51 in). Inputting these values into the equations results in $63.65 > 92.225$ from the first equation and $203.2 > 112.5$ from the second equation. The first result is clearly false, while the second result is true. The equations therefore predict that diagonal cracks will dominate the deck fracture. However, the trial 2 analysis shows that horizontal cracks dominate. This result disagrees with Bažant's assumptions.

Trial 3 has a rebar spacing $s = 101.6$ mm (4 in), and the same bar diameter and concrete cover values as trial 2. Inputting these values into the equations results in $63.65 > 41.425$ from the first equation and $101.6 > 112.5$ from the second equation. In this case the first result is true while the second is false. The equations therefore predict a dominance by the horizontal cracks. However, the trial 3 analysis shows that diagonal cracks dominate the concrete fracture. Again, this disagrees with Bažant's assumptions.

5 Summary and conclusions

Overall, the bridge deck deterioration model succeeds in numerically simulating the three main components of deck deterioration: chloride diffusion, rebar corrosion, and concrete fracture.

Concerning chloride diffusion, the current model presented here assumes fully saturated concrete. This is not always the case, and if thermal loading is included then fully saturated concrete is rarely the case. Future chloride diffusion models must include provisions for unsaturated and partially saturated concrete. The current model also only considers one transport mechanism, so others must be included.

Concerning the rebar corrosion analysis, improvements need to be made on the polarization solution technique. The iterative nature of the solution can be automated in a finite element code, and efforts are currently underway to do this with MERLIN. Alternately, Fu (1982) has shown that polarization follows an expression which is similar to the convective heat transfer equation for solid/fluid interfaces, so this may be used in a corrosion analysis.

Concerning concrete fracture, the fracture analysis method of

trial 1, which involves assumed crack paths, is a straightforward and relatively quick method to determine the time to concrete cracking due to rebar corrosion. However, the assumed crack paths may not be correct for all types of loadings and stresses. The fracture analysis method of trial 2 is an improvement on trial 1 in that no crack path is assumed. This allows for more correct fracture results because the crack paths can be followed in any direction. However, this method is time-consuming due to the numerous analyses that must be performed. The results of trial 3 show that the effects of rebar spacing on crack opening can be captured with these analysis and are consistent with the previous results.

Acknowledgement

E. Hansen wishes to thank GAANN (Graduate Assistance in Areas of National Need) for its support.

References

- Bazant, Z. P.: 1979, Physical model for steel corrosion in concrete sea structures- theory, **Journal of the Structural Division** 105(ST6), 1137-1153.
- Fu, J. W.: 1982, A finite element analysis of corrosion cells, **Corrosion** 38(5), 295-296.
- Hibbit, Karlsson & Sorensen, Inc.: 1995, Abaqus version 5.5-1, Commercial code.
- Hillerborg, A., Modeer, M. and Petersson, P.: 1976, Analysis of crack formation and crack growth in concrete by means of fracture mechanics and finite elements, **Cement and Concrete Research** 6(6), 773-782.
- Jones, D.: 1995, **Principles and Prevention of Corrosion**, Prentice-Hall.
- Mangat, P. and Molloy, B.: 1992, Factors influencing chloride-induced corrosion of reinforcement in concrete, **Materials and Structures** 25(151), 404-411.

- Mangat, P. and Molloy, B.: 1994, Prediction of long term chloride concentration in concrete, **Materials and Structures** 27(170), 338–346.
- Reich, R., Červenka, J. and Saouma, V.: 1994, Merlin, a three-dimensional finite element program based on a mixed-iterative solution strategy for problems in elasticity, plasticity, and linear and nonlinear fracture mechanics, Technical report, University of Colorado, Boulder, Palo Alto.
- Saouma, V.: 1995, Lecture notes in fracture mechanics, Lecture notes, CVEN 6831, University of Colorado-Boulder.
- Tang, L. and Nilsson, L.: 1994, A numerical method for prediction of chloride penetration into concrete structures, **The Modelling of Microstructure and Its Potential for Studying Transport Properties and Durability**, Saint-Rémy-lés-Chevreuse, France.
- Červenka, J.: 1994, **Discrete Crack Modeling in Concrete Structures**, PhD thesis, University of Colorado, Boulder.
- Weyers, R., Fitch, M., Larsen, E., Al-Qadi, I., Chamberlin, W. and Hoffmann, P.: 1994, Concrete bridge protection and rehabilitation: Chemical and physical techniques, Technical report, Virginia Polytechnic Institute and State University, Blacksburg, VA. Strategic Highway Research Program.